Crystallization and thermal behaviour of poly(D(−)-3-hydroxybutyrate)-based blends

Pietro Greco and Ezio Martuscelli*
Istituto di Ricerche su Tecnologia dei Polimeri e Reologia, CNR, Via Toiano 6, 80072 Arco Felice, Napoli, Italy
(Received 4 October 1988; accepted 3 January 1989)

The influence of molecular structure and characteristics of an uncrystallized rubbery second component (ethylene–propylene rubber (EPR) and poly(vinyl acetate) (PVAc)) on the melt miscibility, phase structure, morphology, thermal and crystallization behaviour of blends based on poly(D(−)-3-hydroxybutyrate) (PHB) has been investigated by differential scanning calorimetry and optical microscopy. PHB and EPR are immiscible in the melt, whereas PHB and PVAc are compatible. Consequently PHB–PVAc blends show a single glass transition and a drastic depression of equilibrium melting temperature of PHB. Conflicting results are obtained when the Flory–Huggins and Kwei–Frisch equations are used to describe and analyse this melting-point depression. In PHB–EPR blends no change in the radial growth rate G of PHB spherulites occurs with increasing EPR content. The PHB spherulites grow in the presence of a PHB melt containing EPR domains as the dispersed phase. During growth the EPR particles are first ejected and then occluded in intraspherulitic regions. In the case of PHB–PVAc blends, at a given T_c, G decreases with increasing PVAc content. PHB spherulites grow in equilibrium with a one-phase melt. The phase structure in the solid state is characterized by the presence of a homogeneous amorphous phase situated mainly in interlamellar regions of crystalline PHB and consisting of PVAc molecules and uncrystallized PHB chains.

(Keywords: poly(D(−)-3-hydroxybutyrate; ethylene–propylene copolymer; poly(vinyl acetate); blend; crystallization; miscibility)

INTRODUCTION

The miscibility of poly(D(−)-3-hydroxybutyrate) (PHB) and poly(ethylene oxide) (PEO) was studied by Martuscelli *et al.*[1]. It was found that the components, both crystallizable, are miscible in the melt. Thus the blend exhibits a single glass transition temperature and a depression of the equilibrium melting temperature as well as of the radial growth rate of PHB spherulites. The phase structure of the solid blend, that is after crystallization of components, is characterized by the fact that during the growth of PHB spherulites the PEO molecules diffuse away from the crystallization front to interlamellar and/or interfibrillar regions. Thus, in such regions a homogeneous solution of uncrystallized PHB and PEO molecules is probably formed[1].

In the present paper the results of an investigation concerning the morphology, thermal and crystallization behaviour of blends obtained by mixing PHB with uncrystallized rubbery components, ethylene–propylene rubber (EPR) and poly(vinyl acetate) (PVAc), are reported. The main goal of this study is to find out how the molecular structure and molecular characteristics of a second component may influence and determine the miscibility in the melt and solid state as well as the phase structure and interaction between phases in the case of PHB-based blends. Melt mixing procedures developed in our institute have been used to prepare rubber-modified PHB samples. Such materials are at the moment under investigation in order to assess how the second component may influence the processability window and/or the impact properties of PHB at low temperature.

EXPERIMENTAL

Materials

Molecular characteristics, sources and codes of the polymers used in this paper are reported in *Table 1*. The PHB sample, furnished by ICI, was synthesized by continuous fermentation of a glucose-utilizing mutant of *Alcaligenes eutrophus*[2].

Preparation of blends

Both PHB–EPR and PHB–PVAc blends were prepared by slowly casting films from chloroform. The resulting films were dried under vacuum at 80°C until they reached constant weight. The composition of PHB–EPR and PHB–PVAc blends investigated and the range of crystallization temperatures (T_c) explored are reported in *Table 2*.

Measurements of radial growth rate of PHB spherulites

The radial growth rate $G = dR/dt$ (where R = radius of spherulites and t = time) of PHB spherulites was measured by photographing the spherulites at a given T_c as a function of time during the isothermal crystallization process in an optical microscope. The radial growth rate G was calculated as the slope of the lines obtained by plotting the radius R against the time t. A Reichart

* To whom correspondence should be addressed

0032-3861/89/081475-09$03.00

Table 1 Materials

Polymer	Source	Code	Molecular mass
Poly(D(−)-3-hydroxy butyrate)	ICI (UK)	PHB	$\bar{M}_n = 279\,000^a$
Random ethylene–propylene copolymer (EPR054)	Dutral SpA (Italy)	EPR	$\bar{M}_w = 180\,000$ $\bar{M}_w/\bar{M}_n = 3.9$ E/P ratio = 2.0
Poly (vinyl acetate) (PVAc-K60)	Montedison (Italy)	PVAc	$\bar{M}_n = 231\,000^b$

[a] By g.p.c. in chloroform at 30°C
[b] By intrinsic viscosity measurements in acetone at 25°C by using the equation[17] $[\eta]/(\mathrm{l\,g^{-1}}) = 2.14 \times 10^{-5} M_n^{0.68}$

Table 2 Composition of PHB–EPR and PHB–PVAc investigated and range of crystallization temperature (T_c) explored

Blend composition (weight ratio)	Range of T_c (°C) explored
PHB–EPR	
100/0	120–145
85/15	120–145
70/30	120–145
PHB–PVAc	
100/0	120–145
85/15	115–135
70/30	110–135
50/50	105–135
30/70	90–115

polarizing optical microscope equipped with a Mettler hot stage (precision ±0.2°C) was used.

The standard procedure was the following: Thin films of PHB, PHB–EPR and PHB–PVAc blends, as obtained by casting, were first heated to 190°C and kept at this temperature for 1 min; then the temperature was rapidly lowered to the desired T_c and the PHB allowed to crystallize isothermally. As soon as the spherulites of PHB filled all the space available, that is impingement occurred, the temperature was raised at a rate of 10°C min^{-1} and the melting point of the sample crystallized at T_c was measured optically by detecting the disappearance of the birefringence pattern. During the thermal treatment the blend films were kept under a continuous stream of nitrogen in order to avoid degradation of polymers.

Differential scanning calorimetry and glass transition temperature measurements

The influence of the second component, of the composition and of the thermal history on quantities such as crystallinity, melting and crystallization temperature of PHB was studied using differential scanning calorimetry (d.s.c.). The procedure was the following: The films obtained by casting were heated from −100°C to 200°C (run I). The melting temperature and the crystallinity were determined from the d.s.c. endotherms. After 1 min at 200°C the samples were cooled down to −100°C (crystallization run). The crystallization exotherms and the crystallization temperature were registered.

Finally the samples were heated up to 200°C (run II). The melting point and the crystallinity of polymers after this thermal history were again measured. A scan rate of 20°C min^{-1} was used throughout.

The glass transition temperature T_g of plain polymers and blends was obtained by heating a sample first melted at 200°C and then rapidly quenched at −100°C. A Mettler TA-3000 apparatus, equipped with a control and programming unit (microprocessor TC-10) and a calorimetric cell DSC-30, which allows temperature scans from −170 to 600°C, was used.

RESULTS AND DISCUSSION

Non-isothermal crystallization: calorimetric studies

The d.s.c. thermograms of plain PHB, PHB–EPR and PHB–PVAc samples as obtained by casting show only one endotherm peak when heated from −100 to 200°C (run I). The peak represents the fusion of PHB phase. The apparent melting temperature (T'_m)of PHB (run I), as reported in *Table 3*, decreases with increase of the content of the second component.

The d.s.c. thermogram of plain EPR (see *Figure 1*) is characterized by the presence of the T_g at about −42°C and by two endotherm peaks: the first rather broad between −35°C and 20°C, and the second rather sharp at about 45°C. The overall crystallinity (X_c) is about 6%. This value is obtained according to the well known equation:

$$X_c = \Delta H^*_m / \Delta H_m \qquad (1)$$

where ΔH^*_m is the apparent enthalpy of fusion of the sample and ΔH_m is the thermodynamic enthalpy of fusion of polyethylene, the only crystallizable comonomer in EPR. The endotherm peaks are due to short-range crystallinity of polyethylene sequences. In PHB–EPR blends no evidence of thermal transitions of EPR are found.

Table 3 Observed melting temperature T'_m (°C) (from d.s.c. Run I) for plain PHB and for PHB crystallized from its blends with EPR and PVAc

Blend composition	T'_m (°C)
PHB 100	179
PHB–EPR 85/15	178
PHB–EPR 70/30	174
PHB–PVAc 85/15	174
PHB–PVAc 70/30	173
PHB–PVAc 50/50	172
PHB–PVAc 30/70	172

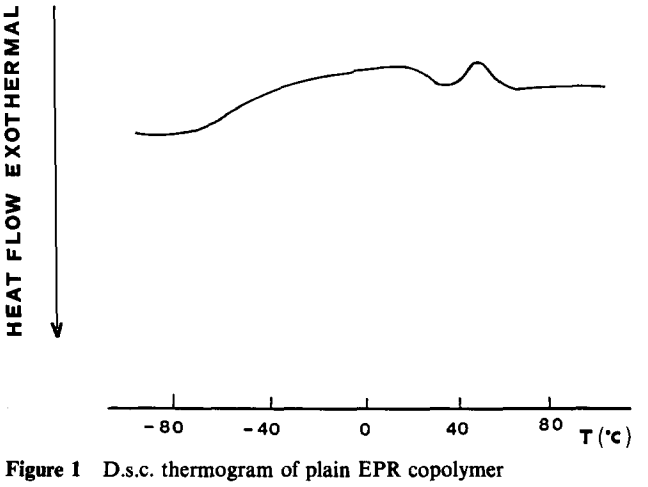

Figure 1 D.s.c. thermogram of plain EPR copolymer

Table 4 Glass transition temperatures (T_g) for PHB–EPR blends

Blend composition	T_g of PHB (°C)	T_g of EPR (°C)
100/0	4	–
85/15	7	−43
70/30	4	−46
0/100	–	−42

Table 5 Glass transition temperatures (T_g) for PHB–PVAc blends

Blend composition	T_g (°C)	T_g from Fox theory (°C)
100/0	4	4
85/15	6	8
70/30	11	13
50/50	15	19
30/70	25	26
0/100	36	36

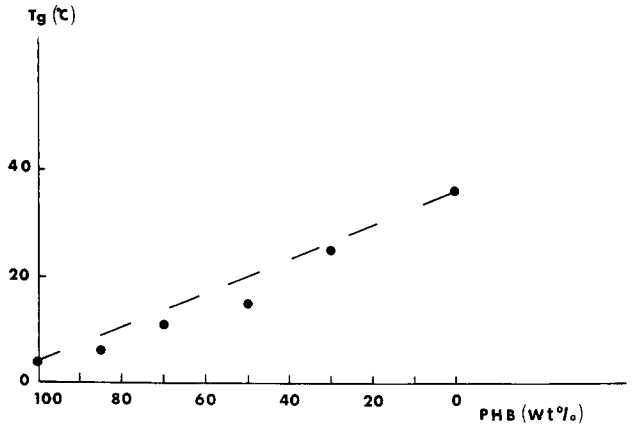

Figure 2 Experimental (●) and theoretical (Fox equation; ———) glass transition temperatures (T_g) for PHB–PVAc blends

The glass transition temperatures (T_g) of PHB, PHB–EPR and PHB–PVAc blends were obtained by d.s.c. measurements. PHB–EPR blends are characterized by two distinct T_g values, as reported in *Table 4*: the first, at about −45°C, of EPR phase, and the second, at about 5°C, of PHB phase. Almost no dependence on composition is observed.

In contrast PHB–PVAc blends are characterized by only one T_g, composition-dependent and intermediate between that of PHB and PVAc (see *Table 5*). As shown by the data reported in *Table 5* and by the graphical representation of *Figure 2*, the values of T_g found experimentally agree quite well with those calculated theoretically using the following Fox equation[3]:

$$\frac{1}{T_g(\text{blend})} = \frac{W(\text{PHB})}{T_g(\text{PHB})} + \frac{W(\text{PVAc})}{T_g(\text{PVAc})} \qquad (2)$$

where T_g(blend) is the glass transition temperature of the blend, T_g(PHB) and T_g(PVAc) are those of plain PHB and PVAc respectively, and W(PHB) and W(PVAc) are the corresponding weight fractions. This finding strongly suggests that PHB and PVAc are compatible in the melt and in the amorphous state.

The d.s.c. thermograms of PHB and PHB–EPR blends obtained during the non-isothermal crystallization run show only one exothermic peak, corresponding to the crystallization of PHB. The temperature position of this peak (T_c), as reported in *Table 6*, is composition-independent.

In contrast for PHB–PVAc blends the T_c and the area of the exothermic peak are drastically influenced by the composition. On lowering the temperature from 200°C to −100°C at a scan rate of 20°C min^{-1}, in the blend samples with a PVAc content of 50% and more, no evidence of a PHB crystallization peak is observed. Such behaviour, as in the case of PHB–PEO[1] and PEO–PMMA[4] blends, is related, as will be discussed in the following paragraphs, to the depression of spherulite growth rate and to the dilution effect of the PVAc component.

The crystallinity of PHB phase, X_c(PHB), and of the blends, X_c(blend), is calculated by the following relations:

$$X_c(\text{PHB}) = \frac{\Delta H^*(\text{PHB})}{\Delta H(\text{PHB})} \qquad X_c(\text{blend}) = \frac{\Delta H^*(\text{blend})}{\Delta H(\text{PHB})} \qquad (3)$$

where ΔH^*(PHB) is the apparent enthalpy of fusion per gram of PHB in the blend; ΔH(PHB) is the thermodynamic enthalpy of fusion per gram of PHB; ΔH^*(blend) is the apparent enthalpy of fusion per gram of blend. The values of X_c(PHB) and X_c(blend) of the cast films, as a function of composition, are reported in *Table 7*. As shown by *Figure 3* the crystallinity of PHB phase is only slightly influenced by blend composition while, as expected, that of blends decreases with the increase of EPR and PVAc content. It is interesting to note that the values of X_c are independent of the chemical nature of the second component.

Isothermal crystallization

Equilibrium melting temperature and melting-point depression. The melting temperature of plain PHB and of PHB crystallized isothermally from its mixtures with EPR and PVAc, measured by optical microscopy, are reported in *Table 8*. For all compositions investigated plots of T'_m against T_c show an almost linear trend for both PHB–EPR and PHB–PVAc blends (see example

Table 6 Non-isothermal crystallization temperature of PHB from its blends with EPR and PVAc

Blend composition	T_c (°C)
PHB 100	86
PHB–EPR 85/15	86
PHB–EPR 70/30	87
PHB–PVAc 85/15	79
PHB–PVAc 70/30	79
PHB–PVAc 50/50	No crystallization observed
PHB–PVAc 30/70	No crystallization observed

Table 7 Overall blend crystallinity (X_c(blend)) and crystallinity of PHB phase (X_c(PHB)) (from d.s.c. run I)

Blend composition	X_c(PHB) (%)	X_c(blend) (%)
PHB 100	62	62
PHB–EPR 85/15	60	51
PHB–EPR 70/30	63	44
PHB–PVAc 85/15	56	48
PHB–PVAc 70/30	57	40
PHB–PVAc 50/50	61	30
PHB–PVAc 30/70	57	17

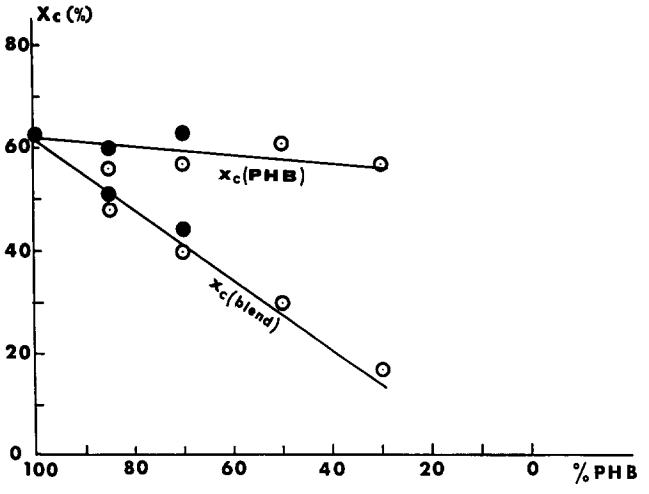

Figure 3 Crystallinity values, X_c(PHB) and X_c(blend), for PHB–EPR (●) and PHB–PVAc (○) blends

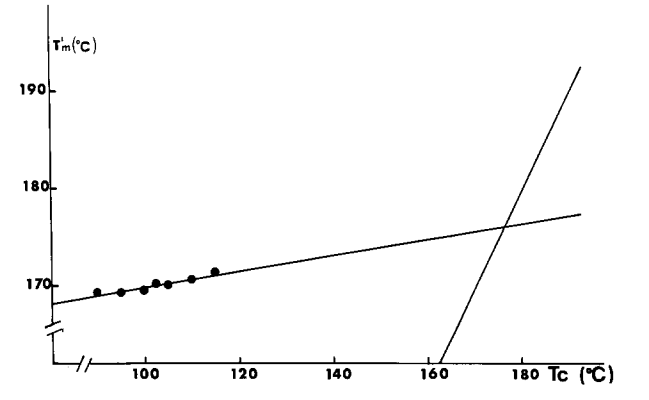

Figure 4 Observed optical melting temperature (T'_m) as a function of crystallization temperature (T_c) for PHB-PVAc 30/70 blend

in *Figure 4*). The Hoffman–Weeks equation[5]:

$$T'_m = T_c/\gamma + (1 - 1/\gamma)T_m \qquad (4)$$

fits the experimental data quite well. Then the extrapolation to the line $T'_m = T_c$ allows the equilibrium melting point T_m to be obtained. The values of T_m determined by this method are reported for each blend in *Table 9* and plotted *versus* EPR and PVAc content in *Figure 5*. For the sake of comparison the T_m value obtained by Martuscelli *et al.*[1] in the case of PHB–PEO blends is also reported.

The value of 196°C found for the equilibrium melting point of PHB agrees quite well with the value of 194°C obtained by Martuscelli *et al.*[1] and with the value of 195°C obtained by Barham *et al.*[6].

From the data of *Table 9* and the trend of *Figure 5* it emerges that the addition of EPR causes a slight depression in the T_m of PHB. On the other hand the addition of PVAc causes a large depression in the T_m of PHB, but not so drastic as PEO.

The thermal behaviour observed for PHB–EPR and PHB–PVAc blends (mainly glass transition and melting temperature dependence on composition) strongly suggests that PHB and EPR are incompatible in the melt and in the amorphous state, while PHB and PVAc are compatible. The melting-point depression of a crystallizable polymer blended with an amorphous one in a

Table 8 Observed melting temperature T'_m for plain PHB and for PHB crystallized isothermally from its blends with EPR and PVAc (from optical microscopy) as a function of crystallization temperature T_c

Blend	T_c (°C)	T'_m (°C)
PHB 100	110.0	174.6
	112.5	173.4
	115.0	173.2
	120.0	175.6
	122.5	176.1
	125.0	177.2
	127.5	177.9
	130.0	178.2
	132.5	179.9
PHB–EPR 85/15	110.0	176.6
	115.0	177.6
	130.0	179.7
	135.0	181.3
	140.0	182.8
	145.0	183.7
PHB–EPR 70/30	110.0	174.5
	112.5	175.6
	115.0	176.9
	120.0	177.5
	122.5	176.7
	127.5	178.5
	130.0	178.7
PHB–PVAc 85/15	115.0	172.4
	120.0	171.9
	125.0	172.9
	127.5	173.0
	130.0	173.4
	132.5	173.5
	135.0	174.7
	140.0	174.3
PHB–PVAc 70/30	105.0	173.0
	107.5	172.1
	110.0	172.1
	115.0	171.8
	117.5	174.2
	120.0	174.0
	125.0	172.0
	127.5	173.2
	130.0	176.0
	135.0	174.5
PHB–PVAc 50/50	105.0	170.0
	107.5	170.1
	110.0	171.4
	112.5	173.6
	115.0	172.9
	120.0	173.8
	125.0	171.3
	130.0	171.5
	135.0	173.8
PHB–PVAc 30/70	90.0	169.2
	95.0	169.3
	100.0	169.7
	102.5	170.1
	105.0	170.2
	110.0	170.6
	115.0	171.4

Table 9 T_m (from optical microscopy) of PHB blends

Blend composition	T_m (°C)
PHB 100	196
PHB–EPR 85/15	193
PHB–EPR 70/30	190
PHB–PVAc 85/15	181
PHB–PVAc 70/30	178
PHB–PVAc 50/50	176
PHB–PVAc 30/70	176

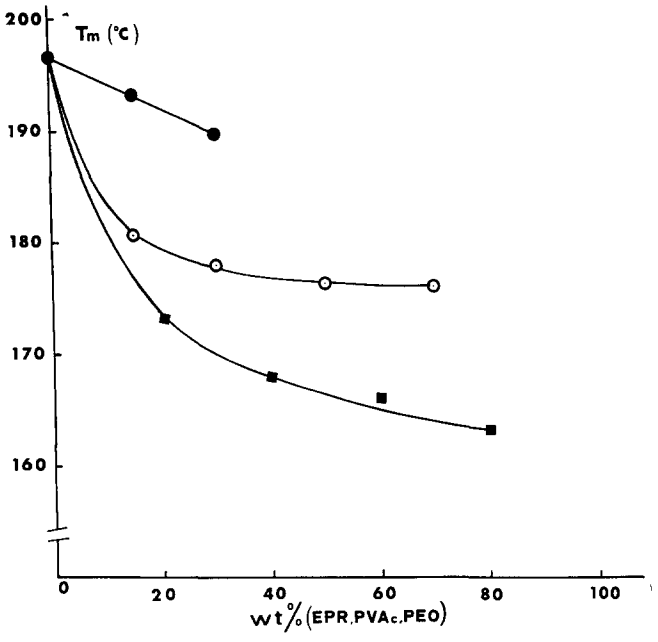

Figure 5 Equilibrium melting temperature (T_m) for PHB–EPR (●), PHB–PVAc (○) and PHB–PEO (■) blends. The upper curve (●) shows melt-incompatible blends, with only a morphological effect on T_m. The lower two curves (○, ■) show melt-compatible blends, with both diluent and morphological effects on T_m

compatible mixture, according to the Flory–Huggins theory[7,8], can be written as:

$$\frac{1}{T_m}-\frac{1}{T_m^\circ}=\frac{RV_2}{\Delta H^\circ V_1}\left[\frac{\ln\phi_2}{m_2}+\left(\frac{1}{m_2}-\frac{1}{m_1}\right)\phi_1+\chi_{12}\phi_1^2\right] \quad (5)$$

where T_m and T_m° are the equilibrium melting points of the blend and homopolymer respectively, ΔH° is the heat of fusion for the 100% crystallizable component, V_1 and V_2 are the molar volumes of the repeat units of non-crystallizable and crystallizable component respectively, and m_1, ϕ_1 and m_2, ϕ_2 are the degree of polymerization and the volume fraction of non-crystallizable polymers. Equation (5) may be applied to PHB–PVAc blends. By rearranging the terms, equation (5) can be written as:

$$-\left[\frac{\Delta H^\circ V_1}{RV_2}\left(\frac{1}{T_m}-\frac{1}{T_m^\circ}\right)+\frac{\ln\phi_2}{m_2}+\left(\frac{1}{m_2}-\frac{1}{m_1}\right)\phi_1\right]=\chi_{12}\phi_1^2 \quad (6)$$

This equation can be used to estimate the PVAc–PHB interaction parameter χ_{12}. If χ_{12} is composition-independent and the melting-point depression is not influenced by morphological effects, then a plot of the left-hand side of equation (6) *versus* ϕ_1^2 should give a straight line passing through the origin. The slope of such a line gives χ_{12}.

In order to calculate the left-hand side of equation (6) the following parameter values have been used: ΔH°(PHB) = 3001 cal mol^{-1}, V_1(PVAc) = 81 cm^3 mol^{-1}, V_2(PHB) = 75 cm^3 mol^{-1}, m_1(PVAc) = 2686 and m_2(PHB) = 3245. For V_1 (molar volume of PVAc) the value of 81 cm^3 mol^{-1} was obtained using the equation[9]:

$$V_1(t)=V_1(25^\circ\text{C})\times(0.823+6.4\times10^{-4}t) \quad (7)$$

where $V_1(25^\circ\text{C})$ is the value of the molar volume of PVAc at 25°C and t is the temperature. $V_1(25^\circ\text{C})$ is 86 cm^3 mol^{-1} and the $V_1(t)$ calculated is the value of the molar volume at 180°C, the temperature at which PHB is in the melt state. For V_2 (molar volume of PHB) the value of 75 cm^3 mol^{-1} was used, which was calculated by using the amorphous density of PHB (1.15 g cm^{-3})[6].

The plot of equation (6) obtained by using the values of T_m°(PHB) and T_m(blend) found experimentally by us (see *Table 9*) is shown in *Figure 6*. The experimental points may be interpolated by a line with an intercept at the origin of 0.12 and a slope of −0.073. The fact that this line does not pass through the origin can be attributed to morphological effects and/or to a composition dependence of χ_{12}. By using the same equation (6) a value of −0.096 was found by Martuscelli *et al.*[1] in the case of the system PHB–PEO.

The equation derived by Kwei and Frisch[10] for non-infinite molecular-weight polymers allows one to calculate C, the proportionality constant for the morphological contributions, and χ_{12}, the interaction parameter:

$$\frac{\Delta H^\circ(T_m^\circ-T_m)}{\phi_1 RT_m^\circ}-\frac{T_m}{m_1}-\frac{\phi_1 T_m}{2m_2}=\frac{C}{R}-\chi_{12}T_m\phi_1 \quad (8)$$

Plotting the left-hand side of equation (8) *versus* ϕ_1 one should obtain a straight line whose intercept at the origin is C/R and whose slope is $-\chi_{12}T_m$.

The results are shown in *Figure 7*. From this one determines for C a value of 653 and for χ_{12} a positive value of +0.8. This finding indicates that part of the melting-point depression must be ascribed to morphological effects that combine with diluent effects. By comparing the two terms on the right-hand side of equation (8), one finds that C/R is greater than $\chi_{12}T_m\phi_1$, and thus it may be concluded that morphological effects strongly influence the melting-point depression of PHB–PVAc blends (see *Table 10*).

The application of equations (6) and (8) to describe analytically the observed melting-point depression of PHB leads to completely different values for χ_{12}. The value of +0.8 found by applying the Kwei and Frisch equation seems to be rather high and probably inadequate to explain the melt miscibility behaviour of PHB–PVAc blends. This finding may be only partly accounted for by a possible composition dependence of χ_{12}. It is likely that the theoretical background on which both equations (6) and (8) are based must be revised in

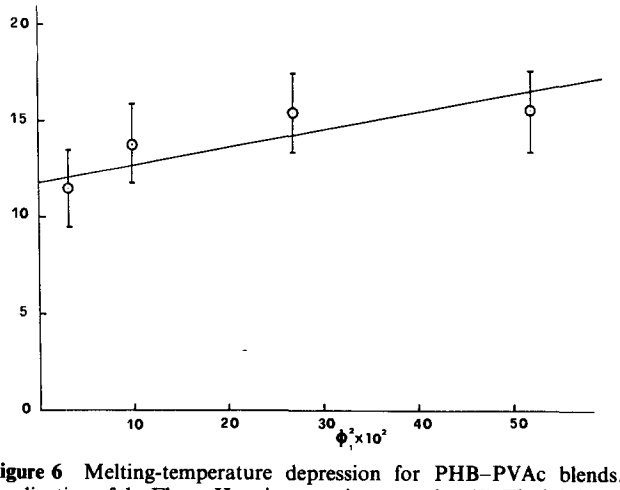

Figure 6 Melting-temperature depression for PHB–PVAc blends. Application of the Flory–Huggins equation, equation (6). The left-hand side of equation (6) (× 10^2) is plotted *versus* ϕ_1^2 (× 10^2)

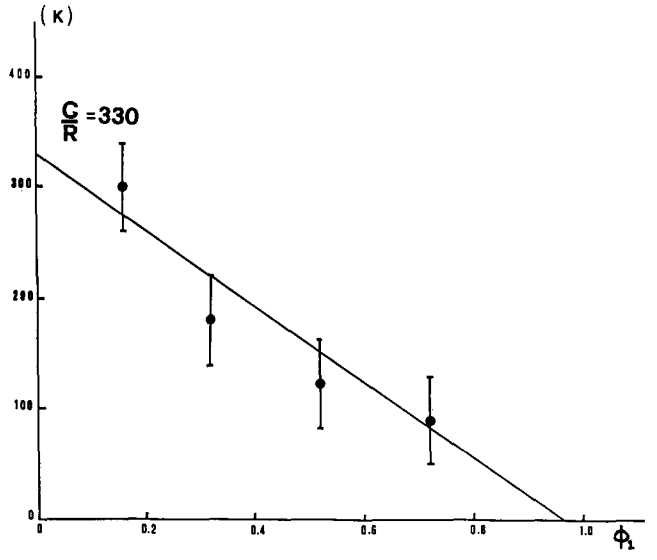

Figure 7 Melting-temperature depression for PHB–PVAc blends. Application of the Kwei–Frisch equation, equation (8). The left-hand side of equation (8) is plotted *versus* ϕ_1

Table 10 Morphological effects and χ_{12} by Kwei and Frisch equation (see text for specification)

Blend composition of PHB–PVAc	C/R	$\chi_{12}T_m\phi_1$	χ_{12} at T_m
100/0	330	0	0.77
85/15	330	58	0.80
70/30	330	116	0.80
50/50	330	188	0.81
30/70	330	261	0.81

the light of the latest equation-of-state theories on polymer–polymer miscibility.

This means that for PHB–PVAc blends the free-volume term, for example, may play an important role in determining the value of χ_{12}. Nevertheless the value of -0.073 found by using equation (6) for the χ_{12} parameter seems to be quite reasonable for the type of thermal and miscibility behaviour shown by PHB–PVAc blends.

Finally it must be said that the extrapolation methods usually followed for the determination of the equilibrium melting point may also introduce some degree of uncertainty in some cases.

Consequently it must be concluded that in the determination of χ_{12} by melting-point depression one must be very critical in the treatment of the data as several different and independent factors may contribute to a χ_{12} value that may not always be reliable.

Radial growth rate of PHB spherulites. As clearly shown by *Figures 8* and *9* in the case of PHB–EPR blends the spherulites of PHB grow in the presence of a two-phase melt. During their growth the spherulites occlude particles of EPR in intraspherulitic regions. For PHB–PVAc blends, at least under our crystallization conditions, the spherulites of PHB grow in equilibrium with a one-phase melt. After crystallization, no apparent evidence of phase separation is observed even when impingement occurs. Nevertheless it can be noticed that the texture of the spherulites is influenced, according to a very complex pattern, by composition (see *Figures 10–13*). It is very likely that, as in the case of PEO–a–PMMA, PEO–s–PMMA and PEO–PVAc, the PVAc molecules are incorporated into interlamellar regions where they form, with uncrystallizable PHB molecules, a homogeneous amorphous phase.

Plots of the radius of PHB spherulites against time result, for all crystallization temperatures and compositions investigated, in straight lines for both PHB–EPR and PHB–PVAc blends. This means that the concentration of PHB crystallizable molecules at the growth front

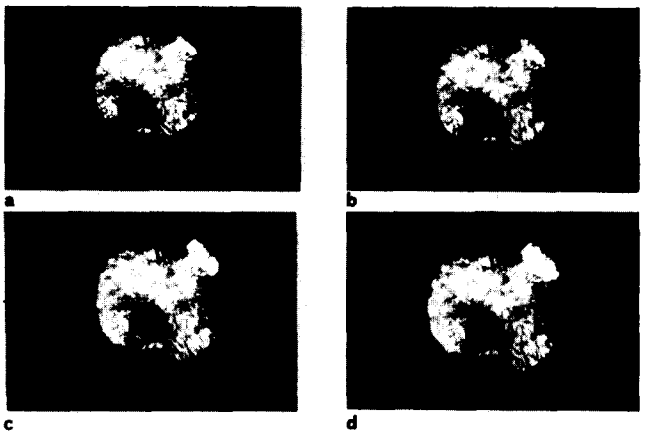

Figure 8 Optical micrographs (crossed polars) of PHB spherulites growing around an EPR liquid domain ($T_c = 115°C$) for PHB–EPR 70/30 blend at different times, t: (a) $t = 4$ min; (b) $t = 6$ min; (c) $t = 8$ min; (d) $t = 10$ min

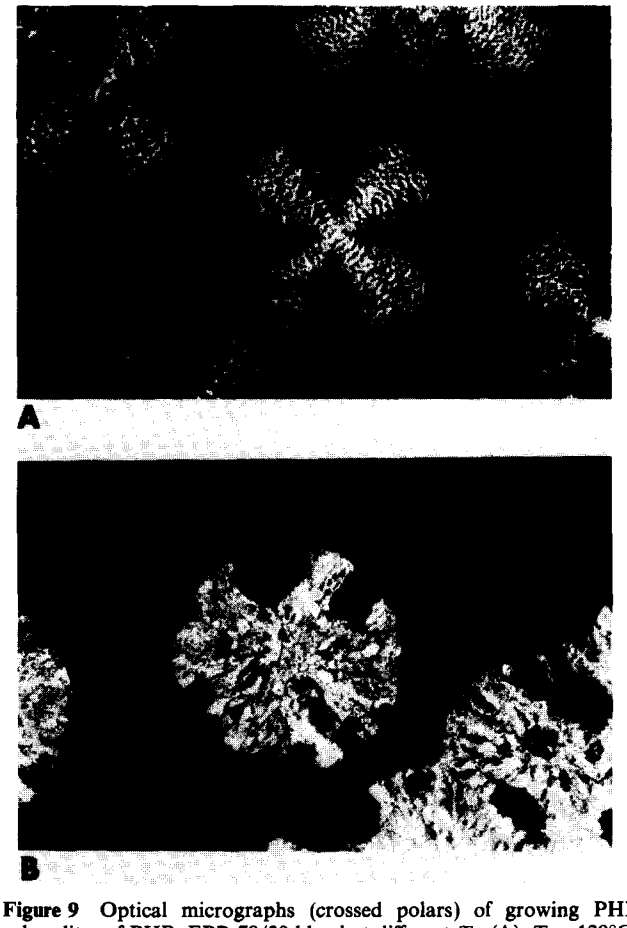

Figure 9 Optical micrographs (crossed polars) of growing PHB spherulites of PHB–EPR 70/30 blend at different T_c; (A), $T_c = 120°C$; (B), $T_c = 145°C$

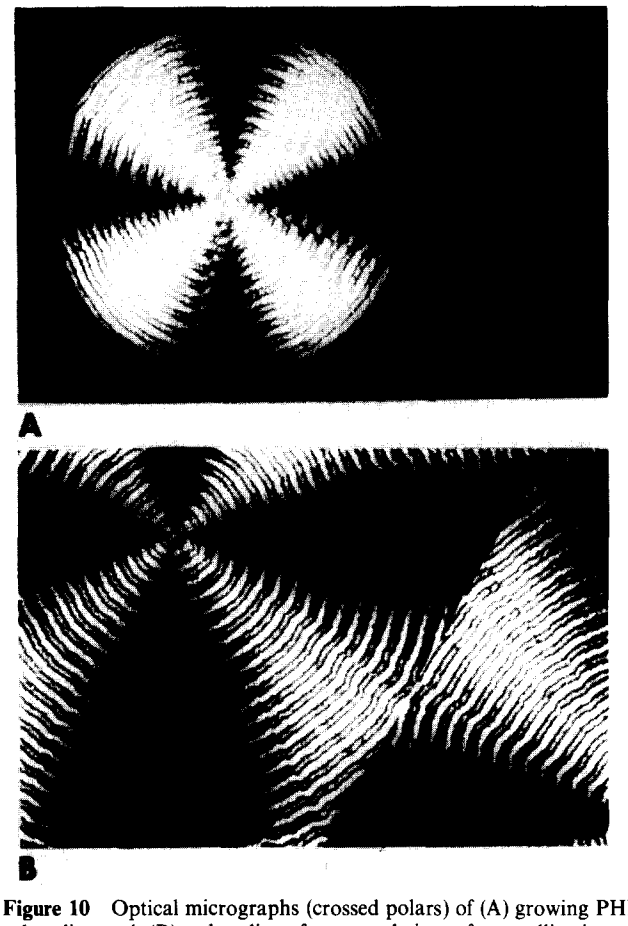

Figure 10 Optical micrographs (crossed polars) of (A) growing PHB spherulite and (B) spherulite after completion of crystallization of PHB–PVAc 85/15 blend at $T_c = 120°C$

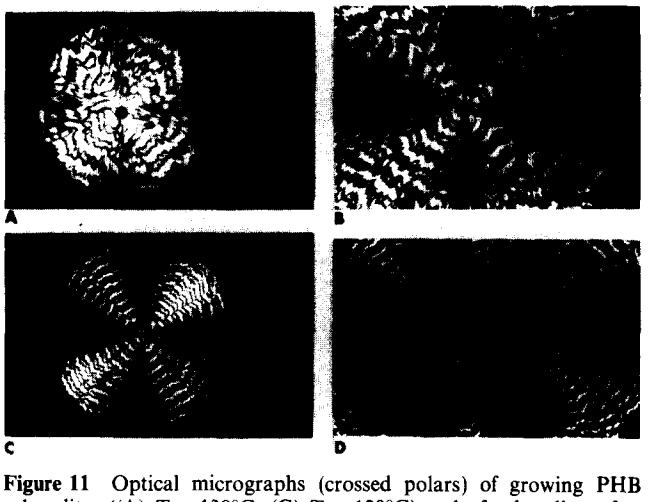

Figure 11 Optical micrographs (crossed polars) of growing PHB spherulites ((A) $T_c = 130°C$; (C) $T_c = 120°C$) and of spherulites after completion of crystallization ((B) $T_c = 130°C$; (D) $T_c = 120°C$) for PHB–PVAc 70/30 blend

is constant during the crystallization process, both in PHB–EPR blends (where PHB and EPR form two quite distinct phases in the melt) and in PHB–PVAc blends (where, on the contrary, PHB and PVAc are compatible in the melt).

The last finding agrees with a growth model characterized by the fact that PVAc molecules diffuse away from the growth front to interlamellar or interfibrillar intraspherulitic regions.

Plots of PHB spherulite radial growth rate G as a function of crystallization temperature T_c for different blend compositions are shown in *Figures 14* and *15* for PHB–EPR and PHB–PVAc blends respectively. From the trend of the curve in *Figure 14* it emerges that the addition of EPR to PHB produces, at a given T_c, no change in the G values. This finding is in agreement with the thermal behaviour and with the morphological observations indicating that in the PHB–EPR melt the EPR component is separated into its own domains. Thus for such blends the PHB spherulites grow in the presence of a two-phase melt.

In the case of PHB–PVAc blends a drastic depression in the G values is observed at a given T_c. As shown by *Figure 15*, the amount of such depression is composition- and temperature-dependent. The depression in G for PHB–PVAc blends is larger at high values of the undercooling (ΔT), while at very low ΔT it tends to vanish (see *Figure 15*). It is interesting to notice that in the case of PHB–PVAc 30/70 blends, G turns out to be independent of T_c, at least for the range investigated (90–115°C) (see *Figure 15*).

As shown by *Figure 16*, at a given T_c, PEO and PVAc give practically the same depression effect on the G of PHB spherulites.

As already discussed in a previous paper[12,13] the spherulite growth rate curves for a polymer–diluent system can be conveniently analysed by using the following growth rate expression[14–16]:

$$\alpha = \log G - \log \phi_2 + \frac{U^*}{2.3R(T_c - T_\infty)} - \frac{0.2T_m \ln \phi_2}{2.3\Delta T}$$

$$= \log G_0 - \frac{K_g}{2.3T_c\Delta Tf} \qquad (9)$$

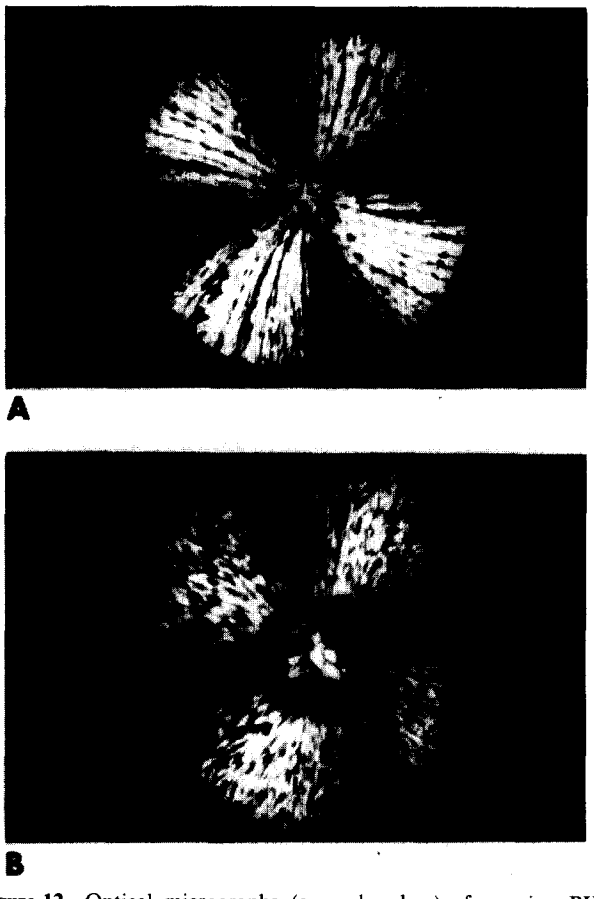

Figure 12 Optical micrographs (crossed polars) of growing PHB spherulite at $T_c = 105°C$ (A) and at $T_c = 110°C$ (B) for PHB–PVAc 50/50 blend

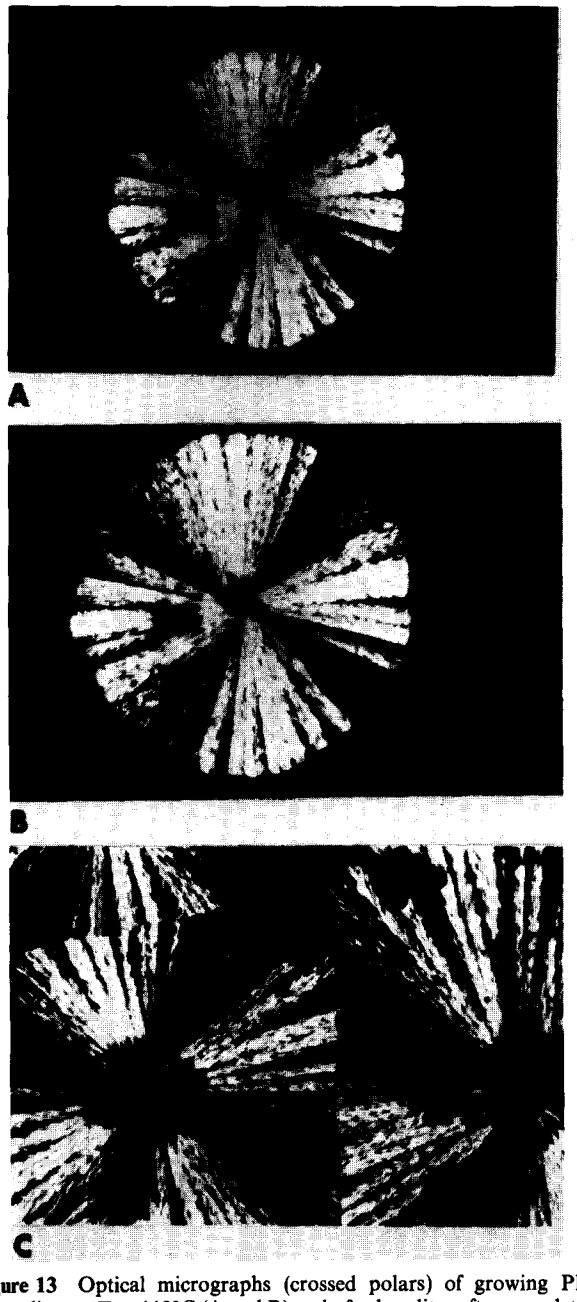

Figure 13 Optical micrographs (crossed polars) of growing PHB spherulites at $T_c = 110°C$ (A and B) and of spherulites after completion of crystallization (C) for PHB–PVAc 30/70 blend

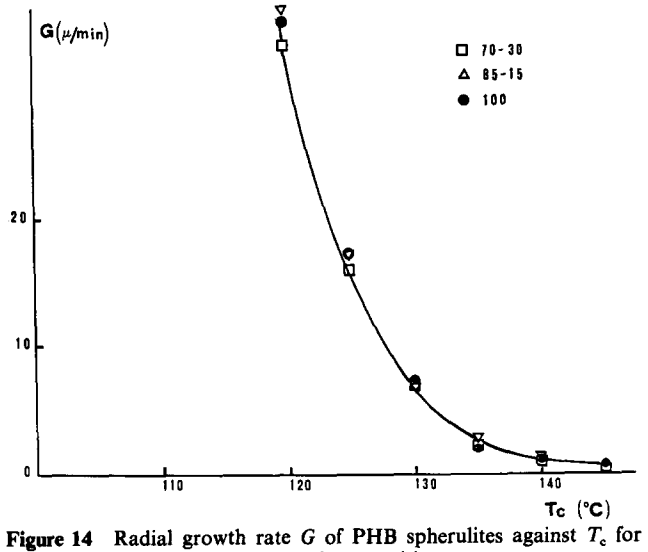

Figure 14 Radial growth rate G of PHB spherulites against T_c for PHB–EPR blends as a function of composition

where G_0 is a pre-exponential factor, ΔT is the undercooling and ϕ_2 is the volume fraction of PHB. The $U^*/R(T_c - T_\infty)$ term contains the contribution of diffusional processes of the crystallizable (PHB) and non-crystallizable (PVAc) components to the growth rate. The quantity U^* represents the sum of the activation energies for the chain motion in the melt of PHB and PVAc molecules. The temperature below which such segmental motion stops is indicated as T_∞ ($T_\infty = T_g - C$)[14]. The quantity f is the correction factor for the heat of fusion, and it takes into account the temperature dependence of $\Delta H°$. Usually the following empirical expression is used for f:

$$f = 2T_c/(T_m^\circ + T_c)$$

K_g is the nucleation factor containing the surface free energies σ and σ_e, equilibrium melting point T_m, heat of fusion $\Delta H°$, thickness of the macromolecular layer b_0 and the Boltzmann constant k:

$$K_g = \frac{nb_0\sigma\sigma_e T_m}{k\Delta H^\circ} \qquad (10)$$

In equation (10), according to Hoffman's theory[14], $n = 4$

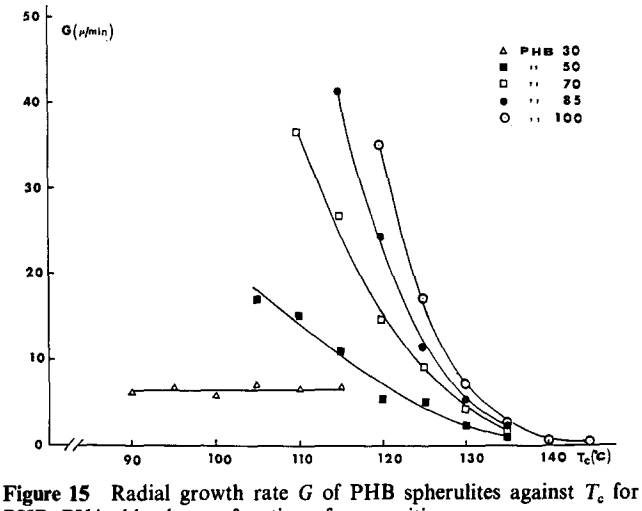

Figure 15 Radial growth rate G of PHB spherulites against T_c for PHB–PVAc blends as a function of composition

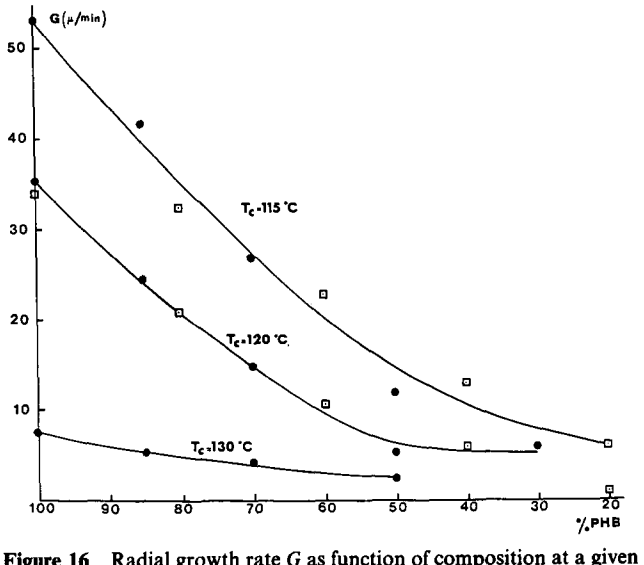

Figure 16 Radial growth rate G as function of composition at a given T_c ($T_c = 115$, 120 and 130°C) for PHB–PVAc (●) and PHB–PEO (□) blends

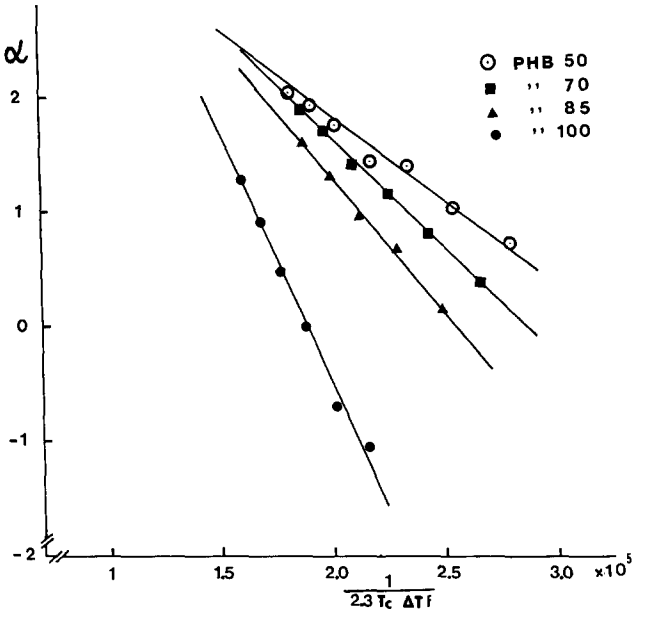

Figure 17 A plot of α given by the left-hand side of equation (9) *versus* $1/(2.3T_c\Delta Tf)$ for PHB–PVAc blends

Table 11 Values of the quantity K_g for plain PHB and PHB–PVAc blends

Blend composition	K_g (K^2)
PHB 100	4.3×10^5
PHB–PVAc 85/15	2.4×10^5
PHB–PVAc 70/30	1.9×10^5
PHB–PVAc 50/50	1.4×10^5

when the crystallization process conforms to regime I (low undercooling) and regime III (very high undercooling). For regime II (intermediate undercooling) n will assume a value of 2.

The procedure for determining K_g involves plotting the left-hand side of equation (9) *versus* $1/(2.3T_c\Delta Tf)$ with the values of U^* and C chosen to give the best-fit least-squares line through the data. A very good fit is obtained when U^* ranges between 1000 and 1500 cal mol^{-1} and $C = 51.6$ K (see *Figure 17*). The values of K_g calculated from the slopes of the lines of *Figure 17* are reported in *Table 11*.

It can be observed that the K_g value of plain PHB is about double the values of 85/15, 70/30 and 50/50 blends. This is in agreement with what was found by Martuscelli *et al.*[1] in the case of PHB–PEO blends.

Barham *et al.*[6] found that PHB crystallizes according to regime III at the undercoolings used in the present work. This means that for PHB in equation (10), $n = 4$. Taking this finding and the data of *Table 11* into consideration, it must be concluded that PHB crystallizes from its blends with PVAc according to regime II, $n = 2$ in equation (10).

CONCLUDING REMARKS

The influence of molecular structure and characteristics of an uncrystallized rubbery second component (EPR and PVAc) on the melt miscibility, phase structure, morphology, thermal and crystallization behaviour of PHB-based blends has been investigated by d.s.c. and optical microscopy. PHB and EPR are immiscible in the melt, whereas PHB and PVAc are compatible. Consequently PHB–PVAc blends show a single glass transition and a drastic depression of equilibrium melting temperature of PHB. Conflicting results are obtained when the Flory–Huggins and Kwei–Frisch equations are used to describe and analyse this melting-point depression. In PHB–EPR blends no change in the radial growth rate G of PHB spherulites occurs with increasing EPR content. The PHB spherulites grow in the presence of a PHB melt containing EPR domains as the dispersed phase. During growth the EPR particles are first ejected and then occluded in intraspherulitic regions according to a mechanism already described by Martuscelli *et al.* in the case of isotactic polypropylene–polyisobutylene and isotactic polypropylene–low-density polyethylene blends[16]. In the case of PHB–PVAc blends, at a given T_c, G decreases with increasing PVAc content. PHB spherulites grow in equilibrium with a one-phase melt. The phase structure in the solid state is characterized by the presence of a homogeneous amorphous phase situated mainly in interlamellar regions of crystalline PHB and consisting of PVAc molecules and uncrystallized PHB chains. The secondary nucleation process is influenced by the presence in the PHB melt of PVAc molecules acting as diluent. According to the latest theory of polymer crystallization, the growth process of plain PHB crystals conforms to regime III, whereas that of crystals growing from a melt blend, at the same T_c, conform to regime II. This last finding is certainly related to the lower melting point of PHB crystallized from blends compared with that of plain PHB.

ACKNOWLEDGEMENT

This work was partly supported by 'Progetto Finalizzato Chimica Fine del C.N.R.'

REFERENCES

1 Avella, M. and Martuscelli, E. *Polymer* 1989, **29**, 1731
2 Hughes, L. and Richardson, K. R. *Eur. Patent Applic.* 1982, **46**, 334
3 Fox, T. G. *Bull. Am. Phys. Soc.* 1956, **2**, 123
4 Addonizio, M. L., Martuscelli, E. and Silvestre, C. *Polymer* 1987, **28**, 183
5 Hoffman, J. D. and Weeks, J. J. *J. Res. NBS* 1962, **66**, 13
6 Barham, P. J., Keller, A., Otun, E. L. and Holmes, P. A. *J. Mater. Sci.* 1984, **19**, 2781; Barham, P. J. *J. Mater. Sci.* 1984, **19**, 3826
7 Flory, P. J., 'Principles of Polymer Chemistry', Cornell University Press, Ithaca, NY, 1953
8 Nishi, T. and Wang, T. T. *Macromolecules* 1975, **8**, 909
9 Brandrup, J. and Immergut, E. H. 'Polymer Handbook', 2nd Edn., New York, 1975
10 Kwei, T. K. and Frisch, H. L. *Macromolecules* 1978, **11**, 1267
11 Silvestre, C., Cimmino, S., Martuscelli, E., Karasz, F. E. and MacKnight, W. J. *Polymer* 1987, **28**, 1190
12 Silvestre, C., Karasz, F. E., MacKnight, W. J. and Martuscelli, E. *Eur. Polym. J.* 1987, **23**, 745
13 Cimmino, S., Martuscelli, E., Silvestre, C., Canetti, M., De Lalla, C. and Seves, A. *J. Polym. Sci., Polym. Phys. Edn.* submitted
14 Hoffman, J. D. *Polymer* 1982, **24**, 3
15 Boon, J. and Azcue, J. M. *J. Polym. Sci. (A-2)* 1968, **6**, 885
16 Martuscelli, E. *Polym. Eng. Sci.* 1984, **24**, 563
17 Moore, W. R. and Murphy, M. *J. Polym. Sci.* 1962, **56**, 519